Egypt. J. Chem. **Vol. 61**, No.5 pp.731 - 746 (2018)

Synthesis, Spectroscopic, Biological and Theoretical Studies of Nano Complexes Derived from Triazine Hydrazone

Fatma Samy[1,2*], A. Taha[2]
[1]*Department of Chemistry, Faculty of Science, University of Tabuk, Saudi Arabia.*
[2]*Department of Chemistry, Faculty of Education, Ain Shams University, Roxy, Cairo 11341, Egypt.*

THE OBJECTIVE of this study is synthesizing of binary and mixed ligands complexes by reacting Co(II), Ni(II), Cu(II) ions with (E)-3-(2-(5,6-diphenyl-1,2,4-triazin-3-yl) hydrazono) butan-2-one oxime (H_2L) in presence and in absence of 8-Hydroxyquinoline ligand. The characterization of complexes is performed by analytical, spectral (IR, mass, UV-Vis, ^{1}H NMR and ESR), magnetic susceptibility, molar conductivity measurements and thermal gravimetric analysis techniques. The scanning electron microscopy is used for detection of the morphology of the ligand and some complexes. The analytical data, spectral studies and magnetic moments established octahedral geometries for all complexes. The ligand behaves as monobasic tridentate ($C=N_{azomethine}$, $C=N_{triazine}$ and OH) for binary complexes. On other hands, The ligand acts as monobasic bidentate ($C=N_{azomethine}$ and OH), for mixed ligands complexes. and mixed ligands complexes, respectively. The optimized structures of the triazine ligand and its complexes theoretically have been done. The structural parameters were correlated with the experimental data. The activity of the triazine ligand and its complexes against Hepatocellular carcinoma, fungi and bacteria have been examined using the diffusion method. The Cu complexes have best activity than the ligand, Co(II) and Ni(II) complexes.

Keywords: Binary and mixed ligands complexes**,** Triazine**,** Monoxime complexes**,** Mixed-ligand**,** Antimicrobial activity.

Introduction

The reaction of nitrogen heterocyclic compounds like triazoles, triazines, imines and amines with aldehydes like substituted and unsubstituted benzaldehyde, salicylaldehyde gave best hydrazones [1,2]. The importance of hydrazone transition metals and lanthanides complexes are in many fields, specifically in agriculture, pharmaceutical and industrial chemistry [3]. Hydrazone ligands and their complexes have important applications as anticancer [4-8], antimalarial [9], antioxidant [10], antimicrobial [11-13], topoisomerase inhibition [14], antihypertensive [15] effect. Some hydrazone compounds act as selective fluorescent for Cu^{2+} [16,17] and Hg^{2+} [16]. On other hands, they exhibit corrosion inhibition [18] and electrochemical properties [19,20]. This work is extension of work on 5,6-Diphenyl-1,2,4-triazine-3-ylhydrazine (DTH) as starting material [1,2, 21-24]. In the present work, Ni(II), Co(II) and Cu(II) complexes of (E)-3-(2-(5,6-diphenyl-1,2,4-triazin-3-yl)hydrazono)butan-2-one oxime (H_2L) in presence and absence of secondary ligand, (8-hydroxyquinoline, 8-HQ) have been synthesized and the characterization and biological applications of the compounds have been examined. The ligand has two important groups, first group is oxime group containing (N & O) donor atoms and second group is triazine ring having N donor atom. The optimized structures of the compounds are carried out and the theoretical data were correlated with the experimental data.

Experimental

Materials and method

Metal salts, $LiOH{\cdot}H_2O$, hydrazine hydrate (100%), thiosemicarbazide, benzil, glacial acetic acid, 8-hydroxyquinoline (8-HQ) and biacetyl monoxime were either Aldrich, BDH or Merck products. Organic solvents were reagent grade chemicals and used without purification.

Synthesis of the triazine ligand

The method in the literature [1] is used to prepare 5,6-Diphenyl-1,2,4-triazine-3-ylhydrazine (DTH). The hydrazone ligand, (E)-3-(2-(5,6-diphenyl-1,2,4-triazine-3-yl)

*Corresponding author e-mail: fatma_chem2000@yahoo.com
DOI:10.21608/ejchem.2018.3798.1326

hydrazono)butan-2-one oxime, H_2L (Scheme 1); was synthesized by dropwise addition of biacetyl monoxime ethanolic solution (1.01 g; 10 mmol) to DTH ethanolic solution (2.63 g; 10 mmol). The mixture was refluxed for 2 h and the hydrazone ligand was filtered off, washed by hot ethanol and dried to give pure yellow product with m.p. 240 ^{o}C; yield 65%.

Synthesis of the binary complexes

Ethanolic solution of the H_2L ligand is refluxed with an aqueous solution of LiOH for ½ hour then metal salt ethanolic solution is added, in molar ratio 1:2:1 (H_2L:LiOH:M) and refluxed for 6-8 h. The binary complexes were precipitated, filtered off, washed with bidistilled water then with EtOH, lastly washed with diethyl ether and complexes are dried in desiccators.

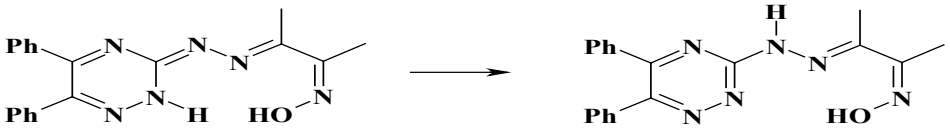

Scheme 1. Tautomeric forms of the ligand.

Synthesis of the mixed ligands complexes

The mixed ligands complexes were prepared by the same method of binary complexes but after ½ hour from the addition of metal, the ethanolic solution of mixed ligands ligand (8-HQ) is added in molar ratio 1:2:1:1 (L:LiOH:M:8-HQ). The precipitate formed after cooling and was separated then dried in vacuum desiccators over anhydrous $CaCl_2$.

Measurements

Elemental analyses were determined using Vario El-Elementar at the Ministry of Defense, Chemical War Department. Stuart melting point instrument is used for measuring the decomposition temperatures of the metal complexes. IR spectra were carried out using KBr discs on a Nicolet 6700 FT IR spectrometer. Electronic spectra were recorded as solutions in DMF on a Jasco UV-Vis spectrophotometer model V-550 UV-Vis. ^{1}H NMR spectra were recorded on a Bruker WP 200 SY spectrometer. Dimethylsulfoxide, DMSO-d6, was used as a solvent and tetramethylsilane as an internal reference. ESR spectra were recorded at an Elexsys, E500, Bruker company. Mass spectra were recorded at 70 eV on a Gas chromatographic GCMSqp 1000 ex Shimadzu instrument. The magnetic susceptibility measurements were carried out at room temperature using a magnetic susceptibility balance of the type Johnson Matthey, Alfa product, Model No. (MKI). Effective magnetic moments were calculated from the relation: $\mu_{eff.} = 2.828 (\chi_M.T)^{1/2}$ B M., where $\chi_{M.}$ eff under, M under and 1/2 up B M., where $\chi_{M.}$ is the molar susceptibility. Molar conductivities of 10^{-3} M solutions of the solid complexes in DMF were measured on the Corning conductivity meter NY 14831 model 441. TG measurements were carried out on a Shimadzu-50 instrument. The SEM is performed to give the morphology for the ligand and some complexes, in FEI company, Netherlands, Model Quanta 250 FEG.

Molecular Orbital Calculations

The optimized structures of complexes and ligand were done by Hyperchem 7.52 program, using semi-empirical (*PM3* level) [25].

Biological studies

The antimicrobial activity of the ligand and its metal complexes was examined against Gram-positive and Gram-negative bacteria and a pathogenic fungus using the disc diffusion technique [26a]. The antitumor activity of the ligand and its metal complexes was carried out against Hepatocellular carcinoma cells (Hep G-2) according to literature technique [26b].

Results and Discussion

In continuation of our ongoing interest to develop the convenient method to isolate a novel compounds, the scheme for the syntheses of complexes is represented in Scheme 2. The formed triazine complexes of the current ligand, H_2L, are powdery solids, colored and stable at normal laboratory temperature. The physical and spectroscopic techniques are performed to characterize the triazine complexes (Tables 1–3). All triazine complexes (Scheme 2) have octahedral geometries. The melting point of all complexes is higher than 300 ^{0}C, except complex (6) which was decomposed at 257 ^{0}C (Table 1). The elemental analysis also maintains the formation in the ratio of 1:1 and 1:1:1 for binary and mixed ligands triazine complexes respectively, for H_2L with Co(II), Ni(II) and Cu(II) ions and 8-HQ (secondary ligand). All complexes are insoluble in most organic solvents, but they dissolve in DMF and DMSO.

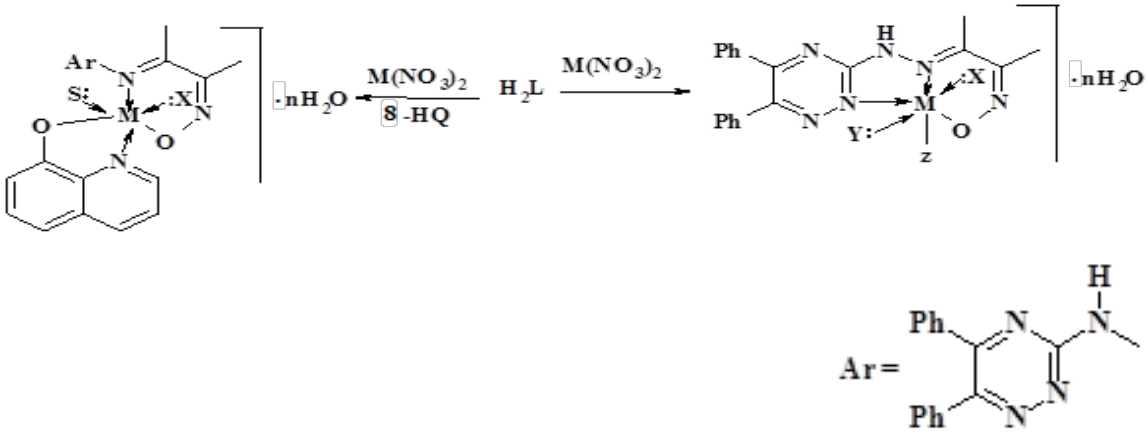

M	X	N	Complex	M	Y	X	Z	n	Complex
Co	EtOH	Nil	4	Co	EtOH	EtOH	NO_3	1½	1
Ni	H_2O	Nil	5	Ni	H_2O	H_2O	OH	nil	2
Cu	EtOH	1	6	Cu	EtOH	H_2O	NO_3	1	3

Scheme 2. Binary and mixed ligands complexes of triazine ligand.

TABLE 1. Analytical and physical data of the ligand and its complexes.

No.	Reactants (H_2L+2LiOH+metal salt)	Complex	F.W.	Color	Yield (%)	Elemental Analysis; % Found/ (Calcd.) C	H	N	M
		H_2L	346.39	Yellow	65	66.11 (65.88)	4.69 (5.24)	24.67 (24.26)	…….
1	Co $(NO_3)_2.6H_2O$	$[Co(HL)(NO_3)(ETOH)_2]$	558.46	Reddish-Brown	78	49.05 (49.47)	4.82 (5.23)	17.22 (17.56)	10.32 (10.55)
2	Ni $(NO_3)_2.6H_2O$	$[Ni(HL)(OH)(H_2O)_2]$	457.13	Reddish-Brown	61	50.66 (49.92)	4.80 (4.85)	18.69 (18.38)	12.75 (12.84)
3	Cu $(NO_3)_2.2.5H2O$	$[Cu(HL)(NO_3)$ $ETOH(H_2O)].H_2O$	553.03	Black	94	45.95 (45.61)	4.89 (4.92)	17.96 (17.73)	11.72 (11.49)
4	Co $(NO_3)_2.6H_2O$ + 8-HQ	$[Co(HL)(EtOH)_2$(8-HQ)].$1½H_2O$	668.64	Brown crystals	78	57.66 (57.48)	4.81 (5.88)	14.52 (14.66)	8.66 (8.81)
5	Ni $(NO_3)_2.6H_2O$ + 8-HQ	[Ni(HL) ETOH)(H_2O) (8-HQ)]	613.34	Dark gray	99	58.99 (58.75)	5.05 (5.26)	16.69 (15.99)	9.40 (9.57)
6	Cu $(NO_3)_2.2.5H2O$ + 8-HQ	$[Cu(HL)(EtOH)_2$(8-HQ)].H_2O	664.24	Dark brown	65	58.08 (57.86)	4.54 (5.77)	14.80 (14.76)	9.41 (9.57)

TABLE 2. Selected IR absorption bands (cm^{-1}) of the ligand, and its complexes.

No.	IR spectra (cm^{-1})								
	v(NH) and/ or v(OH)	v(C=N) azomethine	v(C=N) oxime	v(C=N) triazine	v(N=N) triazine	v(N-N)	v(M–O)	v(M-N)	Other bands
H_2L	3297, 3232	1660	1587	1550	1449	1226	…..	…..	-------
1	3414	1629	1600	1530	1425	1223	562	467	1298, 804; v(NO_3^-) (unidentate)
2	3412	1626	1600	1521	1415	1219	556	443	
3	3411, 3139	1645	1598	1520	1445	1222	556	455	1315, 809; v(NO_3^-) (unidentate)
4	3376, 3191	1639	1604	1576	1466	1225	564	466	1576 m; v(C = N)(8-HQ), 1280 m; v(C-O)phenolic
5	3385, 3199	1639	1602	1578	1467	1226	556	445	1578 m; v(C = N)(8-HQ), 1282 m; v(C-O)phenolic
6	3429	1628	1598	1574	1464	1210	555	467	1574m; v(C = N)(8-HQ), 1278 m; v(C-O)phenolic

TABLE 3. Electronic spectra, molar conductivity and magnetic moment data of the ligand and its complexes.

No.	μ_{eff} (B.M)	Conductance	Electronic spectral bands (nm) DMF [Nujol mulls]	Assignment
H_2L	……..	…….	263, 307	π-π*, n-π*
1	5.09	11.63	290, 346, 440 [252, 347, 501]	intra-ligand, $^4T_{1g}(F) \rightarrow {}^4T_{1g}(P), {}^4T_{1g}(F) \rightarrow {}^4A_{2g}(F)$
2	3.14	4.81	265, 305, 381 [259, 605]	intra-ligand, $^3A_{2g}(F) \rightarrow {}^3T_{1g}(P), {}^3A_{2g}(F) \rightarrow {}^3T_{1g}(F)$
3	1.06	25.7	277, 349, 425 [260, 379, 502]	intra-ligand, LMCT, $[^2T_{2g} \rightarrow {}^2E_g]$
4	5.08	5.45	281, 351, 427, 756 [249, 548]	intra-ligand, $^4T_{1g}(F) \rightarrow {}^4T_{1g}(P), {}^4T_{1g}(F) \rightarrow {}^4A_{2g}(F)$
5	3.07	2.97	280, 350, 437 [207, 271, 348, 502]	intra-ligand, $^3A_{2g}(F) \rightarrow {}^3T_{1g}(P), {}^3A_{2g}(F) \rightarrow {}^3T_{1g}(F)$
6	2.09	16.7	290, 347, 440 [223, 259, 535]	intra-ligand, LMCT, $[^2T_{2g} \rightarrow {}^2E_g]$

Characterization of the triazine ligand

IR spectrum of the ligand exhibits characteristic bands at 1660, 1587, 1550, 1449 and 1226 cm^{-1} (Table 2) which refer to $\nu(C=N)_{Azomethine}$ [27-30], $\nu(C=N)_{Oxime}$, $\nu(C=N)_{Triazine}$, $\nu(N=N)_{Triazine}$ and ν(N-N), respectively [3, 21-23, 27]. The electronic spectrum of the triazine ligand in DMF solution exhibits shoulders at 263 and band at 307 nm could be assigned to π-π* and n-π*, respectively [12,13]. The ^{1}HNMR spectrum of the triazine ligand H_2L, (Fig. 1) in DMSO-d_6 relative to TMS (δ= 0 ppm) showed chemical shifts (δ/ppm) at 2.09 (3H, $CH_3C=NO$, s), 2.23 (3H, $CH_3C=NN$, s), 7.34–7.51 (10 H, two phenyl groups, m) [3, 12,13, 22, 23], 10.87 (1H, OH, s) [28] and 11.43 (1H, NH of hydrazino, s) [3, 22, 23]. The signals due to NH and OH at 11.43 and 10.87 ppm disappeared on deuteration. The mass spectrum of the triazine ligand shows the molecular ion peak at 346.39, that agrees with the formula mass (346.40 amu) deduced from elemental analysis. The SEM for the triazine ligand was recorded (Fig. 2) [31]. The shape of the ligand is Radiated- fibrous. The optimized structure of triazine ligand was determined by hyperchem 7.52 program [25]. Scheme 1 showed the existence of an equilibrium between tautomeric forms (I and II) of the ligand.

IR spectra and conductivity measurements of the complexes

The bands in the region 3429-3139 cm^{-1} (Table 2) of metal complexes assigned to stretching vibrations of NH and OH bonds [32-39]. Stretching vibration frequencies of $\nu(C=N)_{triazine}$ and $\nu(N=N)_{triazine}$ of the ligand are shifted in binary complexes (1-3) to lower wave numbers in the range (1520-1530 cm^{-1}) and (1415-1445 cm^{-1}) respectively, while they are shifted to higher wave numbers in the range (1574-1578 cm^{-1}) and (1464-1467 cm^{-1}), respectively, for mixed ligands complexes (4-6). These findings indicate that: i) The synthesized ligand behaves as monobasic tridentate and bidentate, for binary and mixed ligands complexes, respectively. ii) The hydrazone triazine ligand coordinates to metal complexes *via* (N-triazine, N-azomethine & O-oxime) and (N-azomethine & O-oxime) for binary and mixed ligands complexes, respectively [40-42]. The IR of mixed ligands complexes have new bands in the range (1574-1578 cm^{-1}) and (1278-1282 cm^{-1}), refer to ν(C=N) (8-HQ) and ν(C-O)phenolic, respectively [38&39]. The new bands in the range (1298-1315 cm^{-1}) and (804-809 cm^{-1}) in the IR spectra of nitrate complexes (1 & 3) indicate that nitro group acts as unidentate anion [40, 22]. The IR spectra of the triazine complexes showed new bands in the range (443-467 cm^{-1}) and (555-564 cm^{-1}), which refer to M-N and M-O bond, respectively [35-39]. The molar conductance data of the triazine complexes at room temperature lies in the range 2.97–25.7 ohm^{-1} cm^2 mol^{-1}, which are referring to non-electrolytes nature of the complexes [22-24, 38,39].

Electronic & ESR spectra and magnetic studies of the triazine complexes

The electronic spectral data of triazine complexes in DMF solution as well as in Nujol mulls are presented in Table 3. The UV-Vis spectra showed that L→M charge transfer band obscured the d–d transition bands for most complexes solution [38-41]. The electronic spectra of Cu(II) complexes (3 & 6) in DMF solution show a band at 425 & 440 nm, respectively, corresponding LMCT. However, in Nujol mulls, new band was observed at 502 and 535 nm for $[Cu(HL)(NO_3)ETOH(H_2O)].H_2O$ and $[Cu(HL)(EtOH)_2(8\text{-}HQ)].H_2O$, respectively, which are pointed out $^2E_g \rightarrow {}^2T_{2g}$ transitions [38,39, 43]. The magnetic moment data is 1.06 and 2.09 BM of Cu(II) complexes (3 & 6), respectively, indicating one unpaired electron in this system [29]. Hence, the Cu(II) triazine complexes have a distorted octahedral geometry [42]. The interaction of Cu(II) with neighboring central ions causes lowering magnetic value for complex (3) than expected value of Cu octahedral complexes. The electronic spectra of Ni(II)-complexes (2 & 5) show bands at 381 and 437 nm in DMF solution, which are pointed out CT and $^3A_{2g} \rightarrow {}^3T_{1g}$ (P), whereas in Nujol mulls they show new band at 605 nm for Ni complex (2) and spectrum of Ni complex (5) shows new band at 502 nm, which are pointed out $^3A_{2g}(F) \rightarrow {}^3T_{1g}(F)$. $[Ni(HL)(OH)(H_2O)_2]$ and $[Ni(HL)(ETOH)(H_2O)(8\text{-}HQ)]$, complexes have 3.14 and 3.07 BM, respectively, which refer to two unpaired electrons in octahedral d^8 system [2]. However, the Ni(II) triazine complexes have an octahedral geometry. Absorptions at 440 and (427 & 756) nm in DMF solution, that point out $^4T_{1g} \rightarrow {}^4T_{2g}(F)$ for higher energy and $^4T_{1g} \rightarrow {}^4A_{2g}(F)$ for lower energy transitions, respectively, for $[Co(HL)(NO_3)(ETOH)_2]$ and $[Co(HL)(EtOH)_2(8\text{-}HQ)].1½H_2O$ complexes and absorptions of the Co. Complexes are at 501 and 548 nm in Nujol mulls, that point out $^4T_{1g} \rightarrow {}^4A_{2g}(F)$ transitions [42]. 5.09 and 5.08 BM data of Co(II) complexes (1 & 4) point out high spin octahedral geometry, that refer to the presence of three unpaired electrons in d^7 [23]. Consequently, the magnetic values and UV-Vis spectra (Table 3) of the complexes indicate all complexes have octahedral geometry.

The electronic spectra of H_2L and its triazine complexes in DMF exhibit bands at 263-290, 305-349 and 381-440 nm that refer to $\pi \rightarrow \pi^*$ and $n \rightarrow \pi^*$, intra-ligand charge transfer, respectively. A powder ESR spectra (Fig. 3) of $[Cu(HL)(NO_3)ETOH(H_2O)].H_2O$ and $[Cu(HL)(EtOH)_2(8\text{-}HQ)].H_2O$ at room temperature (Table 4) are characteristic for distorted octahedron geometry [38, 39]. As seen in Table 4 the g// and $g\perp$ values appeared in the 2.045-2.095 and 2.0951-2.152 regions, respectively, which confirmed presence of an unpaired electron in the $d_{x^2-y^2}$ orbitals and $^2B_{1g}$ is the ground state [42]. In general, g// value of the complexes is higher or lower than 2.3, depending on the ionic or covalent nature, respectively. The covalent nature is considered for the Cu(II) complexes (3 & 6), where g// is less than 2.3. The G values are calculated by the expression G = (g// -2)/(g$\perp$ -2) and the G values of complexes (3 & 6) are less than 4 (0.4675 & 0.6248, respectively), referring that interaction of the Cu^{+2} ions [44,45]. These results approve with magnetic moment of the complexes.

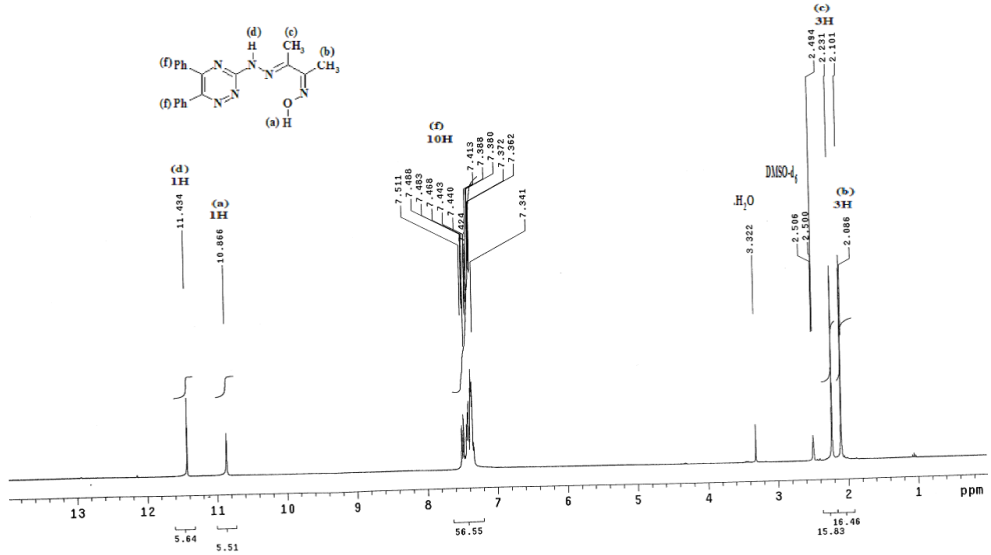

Fig. 1. ^{1}H NMR spectrum of the H_2L, ligand, in DMSO-d_6.

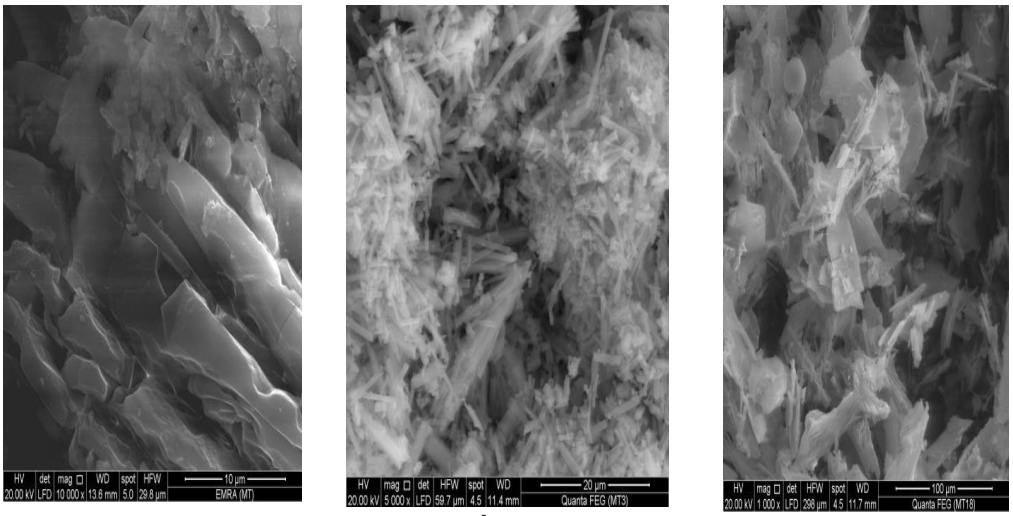

a **b** **c**

Fig. 2. SEM of the ligand (a) and nano Co-complexes (b; 1& c; 4).

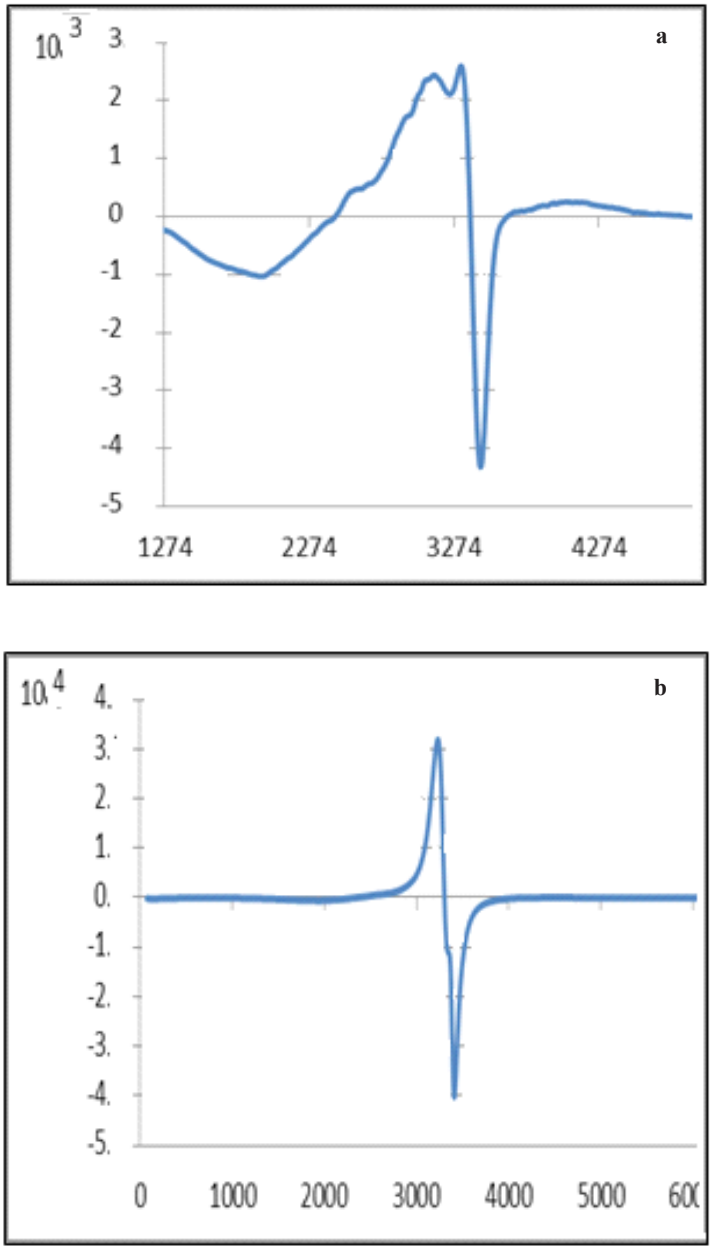

Fig. 3. ESR spectra of Cu- complexes (a; 3 & b; 6) at room temperature.

TABLE 4. ESR data of Cu- complexes at room temperature.

No.	Complex	g_{II}	$g_{\perp}$	g_{iso}	G
3	$[Cu(HL)(NO_3)ETOH(H_2O)].H_2O$	2.04445	2.0951	2.078203	0.467501052
6	$[Cu(HL)(EtOH)_2(8\text{-}HQ)].H_2O$	2.0951	2.1522	2.133167	0.624835742

Thermal Gravimetric analysis of the complexes

Thermal stability and degradation behavior of complexes: $[Cu(HL)(NO_3)ETOH(H_2O)].H_2O$, $[Ni(HL)(ETOH)(H_2O)(8\text{-}HQ)]$ and $[Cu(HL)(EtOH)_2(8\text{-}HQ)].H_2O$ were recognized using thermo gravimetric (TG) technique, the thermal data is recorded in Table 5. The thermogram of $[Cu(HL)(NO_3)ETOH(H_2O)].H_2O$ displays five stages of weight loss in 47-111, 111-255, 255-340, 340-552 and 552 -800 ºC regions. These mass losses are recognized to the elimination of hydrated water (Calcd. 3.25 %, Found 2.98 %), coordinated water [34], EtOH and NO molecules, (Calcd. 17.00%, Found 18.10%), $C_{12}H_{10}$ moiety (Calcd. 27.89%, Found 27.87%), $C_3H_3N_3$; $C_2H_2(OH)_2$ moieties (Calcd. 25.34%, Found 26.04%), and leaving the mixture of $C_2H_3N_2O$ moiety and CuO and carbide residues (Calcd. 26.87%, Found 25.03%). $[Ni(HL)(ETOH)(H_2O)(8\text{-}HQ)].H_2O$ exhibits four TG platforms in the 45-187, 187-346, 346-548 and 548 -800 °C regions. The mass loss indicates the removal of one coordinated water molecule (Calcd. 2.93%, Found 2.68%), ETOH and C_4H_6 (Calcd. 18.28%, Found 17.39%), $C_{14}H_{12}N_6O$ moiety (Calcd. 45.70%, Found 45.26%), the last platform 8-HQ moeity and NiO and carbide residues (Calcd. 33. 07%, Found 34.66%). The thermogram of $[Cu(HL)(EtOH)_2(8\text{-}HQ)].H_2O$ complex shows four TG stages in the 46-88, 88-286, 286-535and 535-800 ºC regions. It also shows elimination of one lattice water molecule (Calcd. 2.71%, Found 2.66%), one coordinated ethanol molecule (Calcd. 13.85%, Found 12.80%), $C_{15}H_{11}N_3$ and Q moieties (Calcd. 56.97%, Found 57.27%), and leaving contaminated mixture of $C_4H_7N_3O$ moiety and residue oxide with carbide. (Calcd. 26.57%, Found 27.27%).

The order (n) and thermo kinetic parameters: activation energy (E_a), enthalpy (ΔH^*), entropy (ΔS^*) and free energy changes (ΔG^*) of the thermal degradation of the complexes are calculated using the Coats–Redfern equations and tabulated in Table 6 [46]. Assessment of the data in Table 6 reveals the following remarks:

The negative values of ΔS^* except the first stage in all investigated complexes indicate that the reactions are slow and/or the reactants are less order than the formed complex [46].

ΔH^* has positive values which point out that the endothermic nature of the decomposition processes. Positive value of ΔG^* mean the thermal decomposition of the complexes are non-spontaneously [2, 22,23].

Mass spectra and SEM of the complexes

The recorded mass spectra for $[Co(HL)(NO_3)(ETOH)_2]$, $[Cu(HL)(NO_3)ETOH(H_2O)].H_2O$, $[Co(HL)(EtOH)_2(8\text{-}HQ)].1½H_2O$, $[Ni(HL)(ETOH)(H_2O)(8\text{-}HQ)]$ and $[Cu(HL)(EtOH)_2(8\text{-}HQ)].H_2O$ complexes have been used to confirm the molecular formula. Figure 4a-b represents the mass spectra of the current binary and mixed ligands cobalt(II)-complexes, $[Co(HL)(NO_3)(ETOH)_2]$ and $[Co(HL)(EtOH)_2(8\text{-}HQ)].1½H_2O$, revealing that the molecular ion peaks (*m/z*) o are: 558.20 and 668.72 respectively, In addition, $[Cu(HL)(NO_3)ETOH(H_2O)].H_2O$, $[Ni(HL)(ETOH)(H_2O)(8\text{-}HQ)]$ and $[Cu(HL)(EtOH)_2(8\text{-}HQ)].H_2O$ complexes showed ,molecular ion peaks at 553.86, , 613.75 and 646.11, respectively, The data obtained agree with the formula weight deduced from elemental analysis for these complexes (Table 1).

TABLE 5. Thermal analyses data (TG) of the H_2L - complexes.

No.	Complex	Temperature range (°C)	%Loss in Wt.		Assignment
			Found	Calc.	
3	$[Cu(HL)(NO_3)ETOH(H_2O)].H_2O$	47-111	2.98	3.25	H_2O (lattice)
		111-255	18.10	17.00	H_2O; EtOH; NO
		255-340	27.87	27.89	phph
		340-552	26.04	25.34	$C_3H_3N_3$; $C_2H_2(OH)_2$
		Above 552	25.03	26.87	Residue, $[CuC_2H_3N_2O]$
5	$[Ni(HL)(ETOH)(H_2O)(8\text{-}HQ)]$	45-187	2.68	2.93	H_2O (coordinated)
		187-346	17.39	18.28	ETOH; C_4H_6
		346-548	45.26	45.70	$C_{14}H_{12}N_6O$
		Above 548	34.66	33.07	Residue, [NiQ]
6	$[Cu(HL)(EtOH)_2(8\text{-}HQ)].H_2O$	46-88	2.66	2.71	H_2O (lattice)
		88-286	12.80	13.85	EtOH (coordinated)
		286-535	57.27	56.97	$C_{15}H_{11}N_3$; HQ
		Above 535	27.27	26.57	Residue, $[CuC_4H_7N_3O]$

TABLE 6. Activation parameters (E*, ΔH*, ΔS* and ΔG*) for the decomposition of the H_2L - complexes.

No.	Stage	N order	DTG peak (°C)	E*	A	ΔH*	ΔS*	ΔG*
3	1st	1	75	68.5816	$5.27*10^9$	67.95835	115.504	59.2955
	2nd	0	239	16.7322	2.929158	14.7461	-71.215	31.7664
	3rd	0	322	17.5241	1.669726	14.84831	-78.362	40.081
	4th	0.66	373	11.4179	0.31132	8.31831	-93.542	43.2093
5	2nd	0	319	21.6658	4.069488	19.01494	-70.882	41.6262
	3rd	1	404	55.6147	3516.874	52.25744	-16.654	58.9856
6	1st	1	58	64.1607	$6.24*10^9$	63.6787	119.048	56.7739
	3rd	1	364	54.2161	4349.25	51.19126	-14.022	56.2954

E* and A are the activation energy and the Arrhenius pre-exponential factor, respectively.

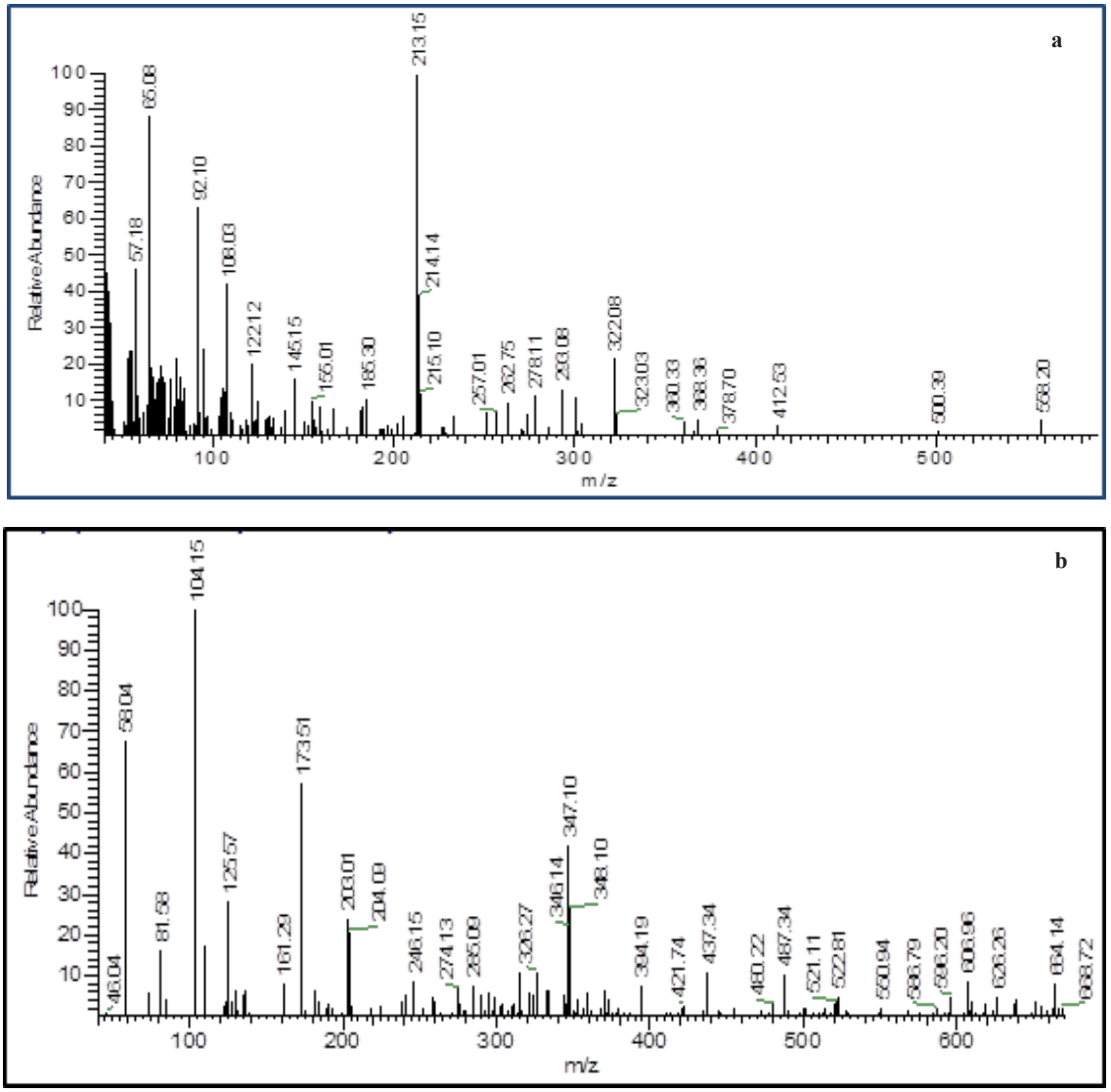

Fig. 4. Mass spectra of the binary and mixed ligands Co complexes (a; 1 & b; 4).

Figure 2 shows SEM of ligand and Co(II) complexes, $[Co(HL)(NO_3)(ETOH)_2]$ and $[Co(HL)(EtOH)_2(8\text{-}HQ)].1½H_2O$. The crystalline size is in nano range (233-455) and (222-379) nm, for Co(II) complexes (1&4), respectively. The shape of the ligand is Radiated- fibrous, which change into Acciuler-needles and Tobular-long prism tetragonal, for nano Co(II) chelates (1&4), respectively.

Molecular Orbital Calculations

The characterization of complexes is performed by analytical, spectral (IR, mass, UV-Vis, ^{1}H NMR and ESR), magnetic susceptibility, molar conductivity measurements and thermal gravimetric analysis (TGA) techniques, which suggested the octahedron geometry for the current complexes. The optimized structure of complexes and ligand are done by Hyperchem *7.52* program, using semi-empirical (*PM3* level). The orbitals (highest occupied molecular orbital and lowest unoccupied molecular orbitals energies), dipole moment and heat of formation are calculated (Table 7). The HOMO orbitals account for the Lewis basicity, whereas LUMO orbitals characterize the Lewis acidity [47].

The molecular stability and reactivity depend on η and $\acute{o}$ values, where hard complexes are less reactive than soft compounds [tautomer I, II and 4], due to electrons transfers to an acceptor [48]. The positive values of electrophilicity index (χ) are point out the compounds can accept electrons from the environment and decreasing its energy upon accepting electronic charge. The heat of formation (Table 7) of the tautomeric form (I) is lower than that of the tautomer (II), refer that the tautomer (II) is less stable than the other. The bond length of $C=N_{azomethine}$ and $(C=N \text{ \& } N\text{-}N)_{triazine}$ bonds (Table 8) are increased than that of the triazine ligand form (I), this point out decreasing the strength of these bonds by complexation.

Table 9 showed best correlations between theoretical and experimental data obtained from *pm3* level, we can conclude the following remarks: 1) The positive slope of the relation between $N_{azomethine}$-M with $\nu(C=N)_{azomethine}$ of the triazine complexes refers to increasing of frequency of $(C=N)_{azomethine}$ bond leading to decreasing frequency of N(azo)-M bond. i.e. increasing of $N_{azomethine}$-M bond length [49]. 2) The negative slope of the relation between length of $C=N_{triazine}$ bond with $\nu(C=N)_{triazine}$ refers to the increasing of $\nu(C=N)_{Triazine}$ leads to decreasing length of $C=N_{Triazine}$ bond. 3) The lengths of $\nu(C=N)_{Triazine}$ or $C=N_{azomethine}$ bonds increase as result of increasing of ν(M-N) and decreasing of λ_{max} of the complexes. 4) The good correlation between $C=N_{Triazine}$ and E_{LUMO} or E_{HOMO} indicates that increasing of E_{HOMO} or decreasing of E_{LUMO} leads to decreasing stability of the triazine complexes, thus the frequencies of $C=N_{Triazine}$ bonds increase. 5) The above calculated data are further emphasized by the correlation between $\nu(C=N)_{azomethine}$ and ΔE_{gap} or E_{HOMO}, where the frequencies of $C=N_{azomethine}$ bonds increase as result of decreasing of ΔE_{gap} and increasing of E_{HOMO}. 6) Increasing of interaction between ligand oxygen and metal leads to increasing of ν(M-O) and decreasing of E_{LUMO}. 7). Increasing of the heat of formation and dipole moment lead increasing of frequencies of M-N bonds [35-39, 49].

Biological activity

Table 10 collects the antitumor activity of the current complexes (1-6) against Hepatocellular carcinoma cells under the experimental conditions. The IC_{50} values are: 62, >500, 177, 6.49, 249, 209 and 6.59 for the triazine ligand and its metal complexes (1-6), respectively indicating that the Cu-complexes (3 & 6) have the lowest IC_{50} values which revealing a pronounced compounds as antitumors [41]. Antimicrobial activity of the triazine ligand and its complexes have been examined against bacteria, Fungi and Yeasts. The ligand and its metal complexes have biological activity, due to the presence of triazine ring. Table 11 showed the following points:

Activity of the triazine ligand increases by complexation [5, 41].

The activity of mixed ligands complexes is higher than that of binary complexes for the same metal ion, due to presence of second ligand (8-HQ) in mixed ligands complexes.

Cu(II) complexes (3 & 6) showed high activity towards *Candida albicans* (ATCC 10231) and *Aspergillus fumigatus*, while binary Co-, Ni-complexes (1 & 2) showed low activity towards that yeast and fungus. On other hands, mixed ligands Co-, Ni-complexes (4 & 5) showed moderate activity toward that yeast and fungus.

Binary Cu(II) complex (3) exhibited moderate activity toward B. subtilis and low activity toward E. coli. mixed ligands Cu(II) complex (6) showed moderate activity toward B. subtilis and E. coli at concentration 1 mg/mL.

TABLE 7. Structural parameters of the ligand and its complexes by *PM3* calculation.

No.	Heat of formation	Dipole moment	[HOMO Energy, [EV	[EV] LUMO Energy,	ΔE_{gap}	global electrophilicity (index ω)	electronegativity (χ)	(global softness (S)	global hardness (η)	softness (σ)
H_2L^a	235.7794	2.216	-7.35311	-1.24078	6.11233	3.056165	0.327207	0.163604	4.296945	3.020736
H_2L^b	275.0922	4.765	-9.16272	-1.73299	7.42973	3.714865	0.269189	0.134594	5.447855	3.994644
1	245464	1722	-7.236663	-6.30286	0.933803	0.466902	2.141779	1.07089	6.769762	49.07852
2	-173.224	5.608	-8.5604	-1.73101	6.82939	3.414695	0.292852	0.146426	5.145705	3.877108
3	-37.2786	9.365	-8.8607	-1.10011	7.76059	3.880295	0.257712	0.128856	4.980405	3.196205
4	242.6444	11.62	-4.52935	-2.40748	2.12187	1.060935	0.942565	0.471282	3.468415	5.669481
5	-139.635	4.416	-8.19631	-0.89988	7.29643	3.648215	0.274107	0.137053	4.548095	2.834971
6	251.4601	5.914	-4.18257	-1.73096	2.45161	1.225805	0.81579	0.407895	2.956765	3.566007

L^a tautomer (**I**^{a}), L^b tautomer (**II**^{b}).

TABLE 8. The selected bond lengths of optimized structures of the ligand and its complexes by *PM3* calculation.

Compound	C=N(azo)	C=N(T)	N-N(T)	O-C	N(azo)-M	N(T)-M	O(oxime)-M
H_2L^a	5.58806	1.38046	1.27515	5.3174	……	……	……
H_2L^b	1.41625	1.42499	1.32124	1.4447	……	……	……
1	1.41824	1.4308	1.34417	1.6274	1.95842	1.97479	1.88605
2	1.44524	1.39285	1.29417	1.20089	1.87084	1.81503	1.83391
3	1.45858	1.44918	1.33741	1.33324	3.96007	1.96549	4.88746
4	1.41286	1.38175	1.27673	1.51359	3.66787	……	2.05733
5	1.16128	1.40116	1.27009	1.22846	1.82008	……	5.43785
6	1.43346	1.43623	1.32428	1.54397	3.20298	……	1.97383

(azo) = azomethene, (T) = Triazine, (S) = solvent = EtOH, (W) = water
HL^a tautomer (**I**^{a}), HL^b tautomer (**II**^{b}). M = Co (**1**&**4**), Ni (**2**&**5**), Cu (**3**&**6**).

TABLE 9. The correlations between experimental values of (UV-VIS & IR) spectra and structural parameters of the complexes.

Equation	R^2	Complexes
Dipole moment = - 110 (14.15) + 0.262 (0.03112) ν(M-N)	98.6	2-4
Heat of formation = - 5030 (410.2) + 11.0 (0.9162) ν(M-N)	99.3	2,3,5
E_{LUMO} = 782 (16.04) - 0.515 (0.01053) ν(C=N)T	100	1-3
E_{HOMO} = - 130 (7.841) + 0.0798 (0.005065) ν(C=N)T	99.2	2-4, 6
E_{HOMO} = 2414 (213.5) - 4.36 (0.3842) ν(M-O)	98.5	2,3,5,6
E_{HOMO} = - 496 (51.99) + 0.300 (0.03187) ν(C=N)azo.	98.9	1,2,4
ΔE_{gap} = 3254 (270.3) - 2.00 (0.1660) ν(C=N)azo.	99.3	1,2,6
ΔE_{gap} = 80.7 (6.257) - 0.134 (0.01110) λ_{max}	99.3	2, 4, 5
(C=N)azo. = - 4.18 (0.1874) + 0.0120 (0.0004063) ν(M-N)	99.8	2, 4-6
(C=N)azo. = 1.97 (0.05495) - 0.000956 (0.00009654) λ_{max}	99	2,4,6
N(azo)-M = - 198 (29.58) + 0.123 (0.01809) ν(C=N)azo.	95.8	1,4-6
(C=N)T = 2.60 (0.2714) - 0.000761 (0.0001759) ν(C=N)T	94.9	1,3,5
(C=N)T = 1.64 (0.07011) - 0.000439 (0.0001243) λ_{max}	92.6	2,4,5
(N-M)ν (0261000.0) 06100.0 + (28370.0) 886.0 = T(N=C)	98	1,2,5,6

(azo) = azomethene, (T) = Triazine

TABLE10. Antitumor activity of the ligand and its complexes against HepG-2.

No.	Compound	IC_{50} (µg/mL)
	Ligand	62
1	$[Co(HL)(NO_3)(ETOH)_2]$	>500
2	$[Ni(HL)(OH)(H_2O)_2]$	177
3	$[Cu(HL)(NO_3)ETOH(H_2O)].H_2O$	6.49
4	$[Co(HL)(EtOH)_2(8\text{-}HQ)].1½H_2O$	249
5	$[Ni(HL)\ ETOH)(H_2O)(8\text{-}HQ)]$	209
6	$[Cu(HL)(EtOH)_2(8\text{-}HQ)].H_2O$	6.59

IC_{50} = inhibition concentration 50%.

TABLE 11. Antimicrobial activity of the ligand and its complexes.

.Mean* of zone diameter nearest whole mm

Organism	Gram - positive bacteria				Gram - negative bacteria				**Yeasts and Fungi			
	Staphylococcus aureus (ATCC 25923)		*Bacillus subtilis* (ATCC 6635)		*Salmonella typhimurium* (ATCC 14028)		*Escherichia coli* (ATCC 25922)		*Candida albicans* (ATCC 10231)		*Aspergillus fumigatus*	
Concentration / Sample	1 mg/ mL	mg/ 0.5 mL	mg/ 1 mL	0.5 mg/ mL	mg/ 1 mL	0.5 mg/ mL	mg/ 1 mL	0.5 mg/ mL	mg/ 1 mL	0.5 mg/ mL	mg/ 1 mL	0.5 mg/ mL
Ligand	-	-	-	-	-	-	-	-	L 9	L 7	-	-
1	-	-	-	-	-	-	I 13	I 12	L 9	L 7	-	-
2	-	-	-	-	-	-	-	-	L 10	L 8	-	-
3	-	-	I 21	I 17	-	-	L 9	L 7	H 27	H 19	H 28	H 20
4	-	-	-	-	-	-	-	-	I 13	I 10	L 8	L 7
5	-	-	-	-	-	-	-	-	I 13	I 10	I 13	I 9
6	L 9	L 7	I 22	H 19	L 10	L 8	I 16	I 13	H 30	H 26	H 33	H 28
# Control	**35**	**26**	**35**	**25**	**36**	**28**	**38**	**27**	**35**	**28**	**37**	**26**

Conclusion

The binary and mixed ligands nano complexes have been synthesized by reacting hydrazino triazine ligand (H_2L) as primary ligand and 8-hydroxy quinolone (8-HQ) as secondary ligand with Co(II), Ni(II) and Cu(II) nitrate salts. The ligand acts as monobasic tridentate, through nitrogen of (azomethine & triazine) and deprotonated oxygen of oxime group, i.e., NNO coordination mode for binary complexes, on other hand it act as monobasic bidentate *via* NO coordination mode for mixed ligands complexes. The IR, UV-vis, ESR and mass spectroscopic techniques are used to characterize the new triazine complexes. The morphology of the triazine ligand and some complexes were detected by SEM. All complexes are non electrolytic and have octahedral geometry. The hyperchem 7.52 program, semiemperical method, (*PM3* level) have been used to optimize the structure of the triazine ligand and its nano complexes. The good correlations were obtained between theoretical and the experimental data (IR and UV-Vis spectra) of the complexes. The activity towered Hepatocellular carcinoma, Bacteria, Fungi and Yeasts have been examined for the

H_2L and its metal complexes. Cu(II)-complexes have good level of inhibitory activity against Hepatocellular carcinoma cells and antimicrobial activity. However, the other triazine complexes have moderate activity. The ligand and its metal complexes have biological activity, due to the presence of triazine ring.

Acknowledgment

The authors would like to acknowledge the financial support for this work from the Deanship of Scientific Research (DSR), University of Tabuk, Tabuk, Kingdom of Saudi Arabia under Grant No. S-1436-0024.

References

1. Taha, A., El-Shetary, B. and Linert, W., Metal chelates of Triazine-Schiff-bases: Complex formation of 3-(á-phenyl)ethylidenehydrazino-5,6-diphenyl-1,2,4-triazine with copper(II), *Monatsh. Chem.,* **124**(2), 135-147 (1993).

2. Taha, A., Farag, A.A.M., Adly, O.M.I., Roushdy, N., Shebl, M. and Ahmed, H.M., Synthesis, spectroscopic, DFT and optoelectronic studies of 2-benzylidene-3-hydroxy-1-(5,6-diphenyl-1,2,4-triazine-3-yl)hydrazine metal complexes, *J. Molec. Struct.,* **1039**, 31-42 (2017).

3. Nfor, E.N., Husian, A., Majoumo-Mbe, F., Njah, I.N, Offiong, O.E., Bourne, S.A., Synthesis, crystal structure and antifungal activity of a Ni(II) complex of a new hydrazone derived from antihypertensive drug hydralazine hydrochloride, *Polyhedron*, **63**, 207-213 (2013).

4. Terzioglu, N. and Gursoy, A., Synthesis and anticancer evaluation of some new hydrazone derivatives of 2,6-dimethylimidazo[2,1-b][1,3,4] thiadiazole-5-carbohydrazide, *Eur. J. Med. Chem.,* **38**, 781-876 (2003).

5. Wardakhan, W.W., El-Sayed, N.N.E. and Mohareb, R.M., Synthesis and anti-tumor evaluation of novel hydrazide and hydrazide-hydrazone derivatives**,** *Acta Pharmaceut.,* **63**(1), 45-57 (2013).

6. Cascioferro, S., Parrino, B., Spanò, V., Carbone, A., Montalbano, A., Barraja, P., Diana, P. and Cirrincione, G., 1,3,5-Triazines: A promising scaffold for anticancer drugs development, *Eur. J. Med. Chem.,* **142***,* 523-549 (2017).

7. Cascioferro, S., Parrino, B., Spanò, V., Carbone, A., Montalbano, A., Barraja, P., Diana, P. and Cirrincione, G., An overview on the recent developments of 1,2,4-triazine derivatives as anticancer compounds, *Eur. J. Med. Chem.,* **142**, 328-375 (2017).

8. Cascioferro, S., Parrino, B., Spanò, V., Carbone, A., Montalbano, A., Barraja, P., Diana, P. and Cirrincione, G., Synthesis and antitumor activities of 1,2,3-triazines and their benzo- and heterofused derivatives, *Eur. J. Med. Chem.,* **142**, 74-86 (2017).

9. Melnyk, P., Leroux, V., Sergheraert, C. *and* Grellier, P., Design, synthesis and in vitro antimalarial activity of an acylhydrazone library, *Bioorg. Med. Chem. Lett.*, **16**(1), 31-35 (2006).

10. Suzen, S., Tekiner-Gulbas, B., Shirinzadeh, H., Uslu, D., Gurer-Orhan, H., Gumustas, M. and Ozkan, S.A., Antioxidant activity of indole-based melatonin analogues in erythrocytes and their voltammetric characterization, *J. Enzyme Inhib. Med. Chem.,* **28**(6), 1143-1155 (2013).

11. Ibrahim, K.M., Zaky, R.R., Abou-El-Nadar, H.M. and Abo-Zeid, S.M., Structural, spectral, DFT and biological studies of (E)-3-(2-(2-hydroxybenzylidene)hydrazinyl)-3-oxo-N-(p-tolyl)propanamide complexes, *J. Mol. Struct.,* **1075**, 71-84 (2014).

12. Adly, O.M.I. and Taha, A., Coordination diversity of new mononuclear ONS hydrazone with transition metals: Synthesis, characterization, molecular modeling and antimicrobial studies, *J. Mol. Struct.,* **1038**, 250-259 (2013).

13. Shebl, M., El-ghamry, M.A., Khalil, S.M.E. and Kishk, M.A.A., Mono- and binuclear copper(II) complexes of new hydrazone ligands derived from 4,6-diacetylresorcinol: Synthesis, spectral studies and antimicrobial activity, *Spectrochim. Acta A*, **126**, 232-241 (2014).

14. Turan-Zitouni, G., Altintop, M.D., Ozdemir, A. Demirci, F., Abu Mohsen, U. and Kaplancikli, Z.A., Synthesis and antifungal activity of new hydrazide derivatives, *J. Enzyme Inhib. Med. Chem.*, **28**(6), 1211-1216 (2013).

15. Tabanca, N., Wedge, D.E., Ali, A., Khan, I.A., Kaplancikli, Z.A. and Altintop, M.D., Antifungal, mosquito deterrent, and larvicidal activity of *N*-(benzylidene)-3-cyclohexylpropionic acid hydrazide derivatives, *Med. Chem. Res.*, **22**, 2602-2609 (2013).

16. Lee, H.Y., Swamy, K.M.K., Jung, J.Y., Kim, G.

and Yoon, j, Rhodamine hydrazone derivatives based selective fluorescent and colorimetric chemodosimeters for Hg^{2+} and selective colorimetric chemosensor for $Cu^{2+,}$ *Sensors and Actuators B*, **182**, 530-537 (2013).

17. Jiang, Z., Tian, S., Wei, C., Ni, T., Li, Y., Dai, L. and Zhang, D., A novel selective and sensitive fluorescent turn-on chemodosimeter based on rhodamine hydrazone for copper ions and its application to bioimaging, *Sensors and Actuators B*, **184**, 106-112 (2013).

18. Singh, P., Singh, A.K. and Singh, V.P., Synthesis, structural and corrosion inhibition properties of some transition metal(II) complexes with o-hydroxyacetophenone-2-thiophenoyl hydrazine, *Polyhedron*, **65,** 73-81 (2013).

19. Mondal, S., Das, C., Ghosh, B., Pakhira, B., Blake, A.J., Drew, M.G.B. and Chattopadhyay, S.K., Synthesis, spectroscopic studies, X-ray crystal structures, electrochemical properties and DFT calculations of three Ni(II) complexes of aroyl hydrazone ligands bearing anthracene moiety, *Polyhedron*, **80**, 272-281 (2014).

20. Tang, Y., Lo, N. and Chen, P., Characterization of a new triazine-derived cupric complex immobilized on carbon electrode via electrografting showing electrocatalytic activities towards hydrogen peroxide, *Electrochem. Communications,* **87**, 44-48 (2018).

21. Taha, A., Adly, O.M.I. and Shebl, M., Reactivity and molecular modeling of new solvatochromic mixed-ligand copper(II) chelates of 2-acetylbutyrolactone and dinitrogen bases, *Spectrochim. Acta A*, **140**, 74-84 (2015).

22. Samy, F., Ramadan, A.A.T., Seleem, H.S. and Taha, A., Binary and mixed ligands copper(II) complexes of new hydrazone ligand: Synthesis, spectral, pH-metric and PM3 studies, *Wulfenia J.,* **22**(3), 147-172 (2015).

23. Samy, F., Ramadan, A.A.T.,Taha, A. and Seleem., H.S., Cobalt(II) and Nickel(II) complexes of hydrazone ligand ({(1E)-1-Aza-2-pyrrol-2-ylvinyl} {5,6-diphenyl(1,2,4-triazin-3-yl)}amine): Synthesis, spectral, pH-metric, antimicrobial and PM3 studies, *Asian J. Chem.,*. **28**(12), 2650-2660 (2016).

24. Seleem, H.S., Ramadan, A.A.T., Taha, A. and Samy F., Unreported Coordination Behavior of A squaric bis (hydrazone) ligand, *Res. J. Chem. sci.,* **1,** 109-116 (2011).

25. Hyperchem version 7.5 Hypercube Inc, (2003).

26. [a] Dharmaraj, N., Viswanathamurthi, P. and Natarajan, K., Ruthenium(II) complexes containing bidentate Schiff bases and their antifungal activity, *Transit. Met. Chem.*, **26**, 105-109 (2001). [b] Mosmann, T., Rapid colorimetric assay for cellular growth and survival: Application to proliferation and cytotoxicity assays, *J. Immunol. Methods*, **65**, 55-63 (1983).

27. Maity, D., Mukherjee, P., Ghosh, A., Drew, M.G.B. and Mukhopadhyay, G., A novel trinuclear nickel(II) complex of an unsymmetrical tetradentate ligand involving bridging oxime and acetylacetone functions, *Inorg. Chim. Acta*, **361**, 1515-1519 (2008).

28. Sutradhar, M., Barman, T.R., Klanke, J.**,** Drew, M.G.B. and Rentschler, E., A novel Cu(II) dimer containing oxime-hydrazone Schiff base ligands with an unusual mode of coordination: Study of magnetic, autoreduction and solution properties, *Polyhedron*, **53**, 48-55 (2013).

29. Bedowr, S., Yahya, R.B. and Farhan, N., Structural characterization of copper (II) tetradecanoate with 2,20-bipyridine and 4,4′-bipyridine to study magnetic properties, *J. Saudi Chem. Society*, **22**, 255-260 (2018).

30. Kumar, K. and Murugesan, S., Synthesis, characterization and anti-bacterial activity of divalent transition metal complexes of hydrazine and trimesic acid, *J. Saudi Chem. Society*, **22**, 16–26 (2018).

31. Saif, M., Aboul-Fotouh, S.M.K., El-Molla, S.A., Ibrahim, M.M., Ismail, L.F.M., Improvement of the structural, morphology, and optical properties of TiO_2 for solar treatment of industrial wastewater, *J. Nanopart Res.***, 141**, 227-1238 (2012).

32. Tabanca, N., Wedge, D.E., Ali, A., Khan, I.A., Kaplancikli, Z.A. and Altintop, M.D., Antifungal, mosquito deterrent, and larvicidal activity of N-(benzylidene)-3-cyclohexylpropionic acid hydrazide derivatives, *Med. Chem. Res.,***22***,* 2602-2609 (2013).

33. Pavelek, L., Ladányi, V., Nec¡as, M., Vallová, S. and Wichterle, K., Dioxouranium complexes with pentadentate s-triazine Schiff base ligands: Synthesis, crystal structure and optical properties, *Polyhedron,* **107**, 89-96 (2016).

34. Wang, Y., Xu, F., Zhang, L., Shi, Z., Xing, Y. and Bai, F., Synthesis, structure, surface photovoltage spectra and photocatalytic activity of transition metal with triazine-pyrazole derivatives, *J. Molec. Struct.,* **1147***,* 281-288 (2017).

35. Uysal, S. and Koç, Z.E., Synthesis and characterization of dopamine substitue tripodal trinuclear [(salen/salophen/salpropen)M] (MCr(III), Mn(III), Fe(III) ions) capped s-triazine complexes: Investigation of their thermal and magnetic properties, *J. Mol. Struct.,* **1109**, 119-126 (2016).

36. Adly, O.M.I., Taha, A. and Fahmy, S.A., Spectroscopic and structural studies of new mononucleating tetradentate Schiff base metal chelates derived from 5-acetyl-4-hydroxy-2H-1,3-thiazine-2,6(3H)-dione and 1,3-diaminopropane, *J. Mol. Struct.,* **1093**, 228-238 (2015).

37. Shebl, M., Khalil, S.M.E., Taha, A. and Mahdi, M.A.N., Structural diversity in binuclear complexes of alkaline earth metal ions with 4,6-diacetylresorcinol, *J. Mol. Struct.,* **1027**, 140-149 (2012).

38. Shebl, M., Khalil, S.M.E., Taha, A. and Mahdi, M.A.N., Synthesis, spectroscopic studies, molecular modeling and antimicrobial activity of binuclear Co(II) and Cu(II) complexes of 4,6-diacetylresorcinol, *Spectrochim. Acta A,* **113**, 356-366 (2013).

39. Shebl, M., Adly, O.M.I., Abdelrhman, E.M. and El-Shetary, B.A., Binary and mixed ligands copper(II) complexes of a new Schiff base ligand derived from 4-acetyl-5,6-diphenyl-3(2H)-pyridazinone: Synthesis, spectral, thermal, antimicrobial and antitumor studies, *J. Molec. Struct.*, **1145**, 329-338 (2017).

40. Nakamoto, K., "*Infrared and Raman Spectra of Inorganic and Coordination Compounds*", fifth ed., John Wiley and Sons, New York (1997).

41. El-Shafiy, H.F. and Shebl, M., Oxovanadium(IV), cerium(III), thorium(IV) and dioxouranium(VI) complexes of 1-ethyl-4-hydroxy-3-(nitroacetyl) quinolin-2(1H)-one: Synthesis, spectral, thermal, fluorescence, DFT calculations, antimicrobial and antitumor studies, *J. Mol. Struct.,* **1156**, 403-417 (2018).

42. Shebl, M., Khalil, S.M.E. and Al-Gohani, F.S., Preparation, spectral characterization and antimicrobial activity of binary and mixed ligands Fe(III), Co(II), Ni(II), Cu(II), Zn(II), Ce(III) and UO2(VI) complexes of a thiocarbohydrazone ligand, *J. Mol. Struct.,* **980**, 78-87 (2010).

43. Cotton, F.A., and Wilkinson, G., "*Advanced Inorganic Chemistry,* A Comprehensive Text", fourth ed., John Wiley and Sons, New York (1986).

44. Hathaway, B.J., and Billing, D.E., The electronic properties and stereochemistry of mono-nuclear complexes of the copper(II) ion, *Coord. Chem. Rev.*, **5,** 143-207 (1970).

45. Hathaway, B.J., A new look at the stereochemistry and electronic properties of complexes of the copper(II) ion, *Struct. Bond.,* **57**, 55-118 (1984).

46. Coats, A.W. and Redfern, J.P., Kinetic Parameters from Thermogravimetric Data, *Nature*, **201**, 68-69 (1964).

47. Taha, A., Spectral, electrochemical and molecular orbital studies on solvatochromic mixed ligand copper(II) complexes of malonate and diamine derivatives, *Spectrochim. Acta A*, **59**, 1373-1386 (2003).

48. Yousef, T.A., Abu El-Reash, G.M., El-Gammal, O.A. and Ahmed, S.F., Structural, DFT and biological studies on Cu(II) complexes of semi and thiosemicarbazide ligands derived from diketo hydrazide, *Polyhedron*, **81**, 749-763 (2014).

49. Gutmanns, V., *"The Donor-Acceptor approach to Molecular interaction",* Blenny Press, New York London (1978).

(*Received* 9/5/2018;
accepted 21/6/2018)

تخليق و دراسات طيفية و بيولوجية و نظرية لمتراكبات نانومتريه مشتقة من هيدرازون ترايزين

فاطمة سامي[١و٢] وعلي طه[٢]
[١]قسم الكيمياء - كلية العلوم - جامعة تبوك - السعودية.
[٢]قسم الكيمياء - كلية التربية - جامعة عين شمس - القاهرة - مصر.

الهدف من البحث تحضير متراكبات ثنائية و مختلطة من تفاعل ايونات الكوبلت و النيكل و النحاس مع ٣-(٢-(٥و٦-ثنائي فنيل-١و٢و٤-ترايزين-٣-يل(هيدرازينوا(بيوتان-٢-اون في وجود و غياب ٨-هيدروكسي كينولين. و تم توصيف المتراكبات بالتحاليل العنصرية و الطيفية (الاشعة تحت الحمراء و المرئية و الفوق بنفسجية و مطياف الكتلة و الرنين النووي المغناطيسي للبرتون و الرنين الحركي للالكترون) و قياس المغناطيسية و التوصيلية الكهربية و التحليل الوزني الحراري. و استخدم المجهر الإلكتروني الماسح للكشف عن الشكل المورفولوجي لعامل التراكب و بعض المتراكبات. و قد اوضحت التحاليل العنصرية والدراسات الطيفية والقياسات المغناطيسية ان جميع المتراكبات لها الشكل هرم ثماني الاوجه. و لوحظ ان عامل التراكب يعمل كأحادي القاعدية ثلاثي الاعطاء او ثنائي الاعطاء للمتراكبات الثنائية و الثلاثية علي التوالي. و وجدت علاقات جيدة بين النتائج العملية (طيفي الاشعة تحت الحمراء و المرئية و الفوق بنفسجية) و النظرية . و تم دراسة النشاط لعامل التراكب و المتراكبات مقابل بعض خلايا سرطان الكبد و الفطريات و البكتريا باستخدام طريقة الانتشار. و اوضحت الدراسة ان متراكبات النحاس لها اعلي نشاط بيولوجي من عامل التراكب و متراكبات النيكل و الكوبلت.